doi: 10.4149/gpb_2025016

LncRNA SOX9-AS1 promotes the development of endometrial cancer by sponging miR-497-5p and upregulating E2F transcription factor 3

Baojin Zeng[1], Jingjing Lin[2], Xiuling Ren[3] and Yali Cheng[3]

[1] *Department of Gynecology, Taizhou Hospital of Zhejiang Province, Taizhou, China*
[2] *Service Center, Taizhou Hospital of Zhejiang Province, Taizhou, China*
[3] *Department of Gynecology, Taizhou Enze Medical Center (Group) Enze Hospital, Taizhou, China*

Abstract. Endometrial cancer (EC) is one of the most prevalent gynecologic malignancies, and long non-coding RNA (lncRNA) SOX9-AS1 has been identified as being upregulated in various cancers, indicating its potential role in driving carcinogenesis. However, the involvement and mechanism of SOX9-AS1 in EC have not been thoroughly investigated. The expression of SOX9-AS1 was assessed using qRT-PCR. The impact of molecular intervention on EC cells was evaluated through cell viability, migration, and invasion assays. Survival probability was analyzed using the Kaplan-Meier method. Bioinformatics predictions, dual-luciferase reporter assays, and rescue experiments were conducted to elucidate the specific competitive endogenous RNA (ceRNA) mechanism of the SOX9-AS1/miR-497-5p/E2F3 axis. SOX9-AS1 expression was significantly upregulated in EC tissues and cells, correlating with poor prognosis in EC patients. Knockdown of SOX9-AS1 inhibited the proliferation, migration, invasion, and glycolysis of EC cells. Mechanistically, miR-497-5p suppressed the proliferation, migration, invasion, and glycolysis of EC by targeting E2F3. Molecular interaction analysis indicate that SOX9-AS1 functions as a molecular sponge for miR-497-5p, thereby increasing E2F3 expression. Our work unveiled a novel mechanism by which SOX9-AS1 promotes EC development, suggesting that targeting the SOX9-AS1/miR-497-5p/E2F3 axis may represent a potential therapeutic strategy for EC.

Key words: SOX9-AS1 — miR-497-5p — E2F3 — Endometrial cancer

Introduction

Endometrial cancer (EC) is one of the most common gynecological malignancies in high-income regions, with approximately 380,000 cases and 89,000 mortalities recorded annually worldwide in 2018 (Bray et al. 2018). The incidence of EC has been rising globally, making it a significant public health concern. Despite advancements in diagnosis and treatment, the underlying molecular mechanisms contributing to the development and progression of EC remain elusive. Moreover, many EC patients are diagnosed at advanced stages without effective therapeutic interventions, resulting in a less than 20% 5-year survival rate (Gupta 2017). A deeper understanding of the molecular mechanisms driving EC progression is crucial for developing targeted therapeutic strategies (Makker et al. 2021; Crosbie et al. 2022).

Long non-coding RNAs (lncRNAs) have been acknowledged as critical regulators of gene expression, playing a role in the progression of various cancers, including EC (Gonzalez-Bosquet et al. 2022; Lv et al. 2022; Shan et al. 2022). The lncRNA SOX9-AS1 (SOX9-AS1) has been reported to exhibit an upregulation pattern in intrahepatic cholangiocarcinoma (Wu L et al. 2022) and breast cancer (Wu XP et al. 2022), implying its potential oncogenic activities in carcinogenesis.

Correspondence to: Jingjing Lin, Service Center, Taizhou Hospital of Zhejiang Province. No. 150 Ximen Road of Linhai City, Taizhou, China, 317000
E-mail: LINJJ08@163.com

Nonetheless, the functional role of SOX9-AS1 in EC remains to be explored.

Glycolysis is a hallmark of cancer metabolism, with many cancer cells preferentially relying on this metabolic process even in the presence of oxygen, a phenomenon known as the Warburg effect (Vander Heiden et al. 2009). Although aerobic glycolysis is a less efficient method of obtaining energy compared to oxidative phosphorylation in mitochondria (Vander Heiden et al. 2009; Ganapathy-Kanniappan and Geschwind 2013; He et al. 2022), enhanced Warburg effects facilitates cell proliferation and metastasis of malignant cells by supplementing intermediate metabolites for DNA precursor synthesis and producing a large amount of lactate to induce changes in the tumor microenvironment (Barba et al. 2024).

In the current investigation, we explored the function and underlying mechanisms of SOX9-AS1 in regulating the malignancy of EC cells. Our findings indicated that SOX9-AS1 facilitates cell proliferation, migration, invasion, and glycolysis in EC cells. SOX9-AS1 functions as a molecular sponge to suppress the activity of miR-497-5p, a tumor-suppressive microRNA (miRNA). The inhibition of miR-497-5p results in an increased expression of E2F transcription factor 3 (E2F3) which acts as an oncogenic factor to promote the malignant phenotype of EC cells. Our findings are consistent with the recognized pro-tumorigenic roles of E2F3 in different cancers (Cao et al. 2022; Nie et al. 2022; Zhao et al. 2022), suggesting that targeting the SOX9-AS1/miR-497-5p/E2F3 axis may represent a potential therapeutic strategy for EC.

Materials and Methods

Reagents

Dulbecco's modified Eagle's medium (DMEM) and fetal bovine serum (FBS) were obtained from Gibco (Rockford, USA). TRIzol reagent was sourced from Life Technologies Corporation (Carlsbad, USA). The Click-iT® EdU Imaging Kit, First Strand cDNA Synthesis Kit, and Lipofectamine 3000 were provided by Thermo Fisher Scientific, Inc. (Waltham, USA). The radio immunoprecipitation assay (RIPA) buffer was purchased from Beyotime Biotechnology (Shanghai, China). The Dual Luciferase Reporter Assay Kit was obtained from Promega (Fitchburg, USA). The Cell Counting Kit-8 (CCK8) assay kit was supplied by Dojindo Corp (Kyushu, Japan). Matrigel was acquired from BD Biosciences (New Jersey, USA). The Glucose Uptake Colorimetric Assay kit, Lactate Assay Kit II, and ATP Colorimetric Assay kit were obtained from Biovision (Milpitas, USA). The Universal SYBR Green Master Mix was sourced from Roche (Shanghai, China). An antibody against LDHA was obtained from Cell Signaling Technology (Danvers, USA), while antibodies against HK2, E2F3, and GAPDH were supplied by Abcam (Cambridge, USA).

Public dataset collection and analysis

We accessed and analyzed data from The Cancer Genome Atlas (TCGA) database (https://portal.gdc.cancer.gov/) to investigate lncRNA SOX9-AS1 expression in EC. The transcriptomics data were obtained for 551 EC tissue samples and 35 normal endometrial tissue samples. Raw count data for SOX9-AS1 were extracted using the TCGAbiolinks R package (version 2.22.1). Expression values were normalized using the trimmed mean of M-values (TMM) method and log2-transformed to account for differences in library size and to stabilize variance. To ensure data quality, we applied the following inclusion criteria: samples with a RNA integrity number (RIN) > 7 and a minimum of 10 million mapped reads. Clinical data, including patient demographics, tumor stage, and survival information, were also retrieved for subsequent survival analyses based on the median expression value of SOX9-AS1.

Cells and cell culture

EC cell lines (HEC1A, HEC1B, Ishikawa, RL95-2, and KLE) and human normal endometrial fibroblast cells (hTERT-immortalized HESC) were obtained from the American Type Culture Collection (Manassas, VA, USA). All cell lines were authenticated by short tandem repeat (STR) profiling and tested for mycoplasma contamination before use. Cells were maintained in DMEM (Gibco) supplemented with 10% FBS (Gibco), 100 μg/ml streptomycin, and 100 U/ml penicillin (Gibco). Cultures were incubated under standard conditions of 37°C, 5% CO_2, and 95% relative humidity in a humidified incubator. Cells were passaged using 0.25% trypsin-EDTA (Gibco) when they reached 80–90% confluence, and media was changed every 2–3 days. All experiments were performed using cells between passages 5 and 15 to ensure consistency and reproducibility.

qRT-PCR

Total cellular RNA was extracted using TRIzol reagent (Life Technologies Corporation, Carlsbad, USA) according to the manufacturer's instructions. RNA quality and quantity were assessed using standard spectrophotometric methods. Reverse transcription was performed using the First Strand cDNA Synthesis Kit (Thermo Fisher Scientific, Inc., Waltham, USA) following the manufacturer's protocol. The expression levels of target RNAs were then determined using the Universal SYBR Green Master Mix (Roche, Shanghai, China) on a 7500 Fast Real-Time PCR system (Applied Biosystems, USA). Each biological sample was run in triplicate. Expression levels were normalized against the reference controls of GAPDH (for mRNA and circRNA) or U6 (for miRNA). Relative expression was calculated using the $2^{-\Delta\Delta Ct}$

method. The PCR cycling conditions were as follows: initial denaturation at 95°C for 30 s, followed by 40 cycles of 95°C for 5 s and 60°C for 30 s. Melt curve analysis was performed to ensure specific amplification. The sequencing primers were as follows: SOX9-AS1: 5'-CCATGGAGGCATGGTATCCG-3', 5'-CGCTTGGCAATCTTCAGACG-3'; GAPDH: 5'-GGAGCGAGATCCCTCCAAAAT-3', 5'-GGCTGTTGTCATACTTCTCATGG-3'; miR-497-5p: 5'-GCGCAGCAGCACACTGTG-3', 5'-AGTGCAGGGTCCGAGGTATT-3'; E2F3: 5'-AGAAAGCGGTCATCAGTACCT-3', 5'-TGGACTTCGTAGTGCAGCTCT-3'; U6: 5'-GCTTCGGCAGCACATATACTAAAAT-3', 5'-CGCTTCACGAATTTGCGTGTCAT-3'.

Cell transfection

The short hairpin RNA targeting SOX9-AS1 (sh-SOX9-AS1) and its negative control (sh-NC), miR-497-5p mimic and its negative control (miR-NC), miR-497-5p inhibitor and its negative control (NC inhibitor), E2F3 overexpression plasmid (pcDNA3.1-E2F3) and the control empty pcDNA3.1 vector were all synthesized and provided by GenePharma (Shanghai, China). The short hairpin RNA targeting SOX9-AS1 (sh-SOX9-AS1): 5'-GCTGCACCTATCAACCCATTA-3; 'sh-NC: 5'-AGCTTCACCGATCCAATCCAT-3'; miR-497-5p mimicGuide Strand: 5'-CAGCAGCACACUGUGGUUUGU-3'; Passenger Strand: 5'-CAAACCACAGUGUGCUGCUG-3'; negative control (miR-NC): 5'-CUGUACUCAUGCAGCAGUGAC-3', 5'-CACUGCUGCAUGAGUACAGUC-3'; miR-497-5p inhibitor: 5'-ACAAACCACAGUGUGCUGCUG-3; 'negative control (NC inhibitor): 5'-CUGUCAGACAUCGGACUUGGA-3'. These constructs were transfected into HEC1A and HEC1B cells using Lipofectamine 3000 reagent (Thermo Fisher Scientific) according to the manufacturer's instructions. Briefly, cells were seeded in 6-well plates and grown to 70–80% confluence before transfection. For each well, 2.5 μg of plasmid DNA or 50 nM of miRNA mimic/inhibitor was mixed with 5 μl of P3000™ Enhancer Reagent and 3.75 μl of Lipofectamine 3000 Reagent in 250 μl of Opti-MEM® Medium (Gibco, Rockford, USA). The transfection mixture was incubated at room temperature for 15 minutes before being added dropwise to the cells. The culture medium was replaced with fresh DMEM containing 10% FBS after 6 hours of transfection. Transfection efficiency was verified by qRT-PCR 48 hours post-transfection. All subsequent experiments were performed 48–72 hours after transfection.

EdU (5-ethynyl-2'-deoxyuridine) cell proliferation

To assess cellular proliferation, the Click-iT® EdU Imaging Kit (Thermo Fisher Scientific) was used to detect the percentage of cells actively synthesizing DNA. Cells of interest were seeded onto coverslips and cultured overnight. A 20 μM EdU labeling solution was prepared by diluting the stock in DMEM. After removing half of the culture medium, sufficient EdU solution was added to cover the cells, followed by a 2-hour incubation at 37°C in a humidified environment. The EdU solution was then discarded, and cells were washed twice with PBS. Fixation was performed using 3.7% formaldehyde in PBS for 10 minutes at room temperature, followed by permeabilization with 0.5% Triton® X-100 in PBS. Subsequently, cells were incubated in Click-iT® reaction cocktail, subjected to antibody labeling, and stained with 1×Hoechst® 33342 solution. Fluorescence microscopy was employed to visualize the EdU-labeled cells. Quantification was conducted using ImageJ software, where blue-stained nuclei (representing total cells) and red-stained nuclei (indicating proliferating cells) were counted separately. Five random microscopic fields from each sample were used for quantification of Edu-positive cells.

Cell viability

Cell viability was assessed using the Cell Counting Kit-8 (CCK-8) assay kit (Dojindo Corp, Kyushu, Japan). Briefly, HEC1A and HEC1B cells were seeded in 96-well culture plates at a density of 2,000 cells *per* well in 100 μl of complete DMEM. After incubating cells for 24, 48 or 72 hours, 10 μl of CCK-8 reagent was added to each well. The plates were then incubated for 4 hours at 37°C in a humidified atmosphere with 5% CO_2, protected from light. Following incubation, the absorbance of the solution was measured using a microplate reader (BioTek Elx800; BioTek Instruments, Inc., Winooski, US) at a wavelength of 450 nm. Each biological condition was run in triplicate, and the average recording of the three replicates was determined as the reading of each condition for data analysis.

Transwell migration and invasion assays

Transwell migration and invasion assays were performed using Transwell chambers with 8 μm pore size polycarbonate membranes (Corning Costar, New York, USA). For the invasion assay, the membrane was coated with Matrigel (BD Biosciences, New Jersey, USA) diluted 1:8 in serum-free DMEM (Gibco, Rockford, USA) and allowed to gel at 37°C for 2 hours. For the migration assay, the membrane was left uncoated. HEC1A and HEC1B cells (5×10^4 for migration, 1×10^5 for invasion) in 200 μl serum-free DMEM were seeded onto the top chamber of the Transwell. The bottom chamber was filled with 600 μl DMEM supplemented with 10% FBS (Gibco, Rockford, USA) as a chemoattractant. After incubation for 24 hours at 37°C in a humidified atmosphere with 5% CO_2, non-migrated/non-invaded cells on the upper

surface of the membrane were gently removed with a cotton swab. The cells that had migrated or invaded through the membrane were fixed with 4% paraformaldehyde for 15 min and stained with 0.1% crystal violet for 15 min at room temperature. The stained cells were then counted in five random fields under a light microscope (Olympus, Tokyo, Japan) at 200× magnification.

Cellular glycolysis measurements

The glucose consumption, lactate production, and ATP levels were investigated using the Glucose Uptake Colorimetric Assay kit, Lactate Assay Kit II, and ATP Colorimetric Assay kit, respectively (all from Biovision, Milpitas, USA), according to the manufacturer's protocols. For glucose consumption, HEC1A and HEC1B cells were seeded in 96-well plates (1×10^4 cells/well) and cultured in glucose-free DMEM (Gibco, Rockford, USA) for 1 hour before the assay. Glucose uptake was initiated by adding 100 μM 2-deoxyglucose for 30 min. The cells were then lysed, and glucose uptake was measured at 412 nm using a microplate reader (BioTek Elx800; BioTek Instruments, Inc., Winooski, USA). For lactate production, cells were seeded in 6-well plates (5×10^5 cells/well) and cultured for 24 hours. The culture medium was then collected and deproteinized using a 10 kDa molecular weight cut-off filter. Lactate levels were measured at 450 nm using the microplate reader. For ATP measurement, cells were seeded in 6-well plates (5×10^5 cells/well) and cultured for 24 hours. The cells were then lysed, and ATP levels were determined by measuring the absorbance at 570 nm using the microplate reader. All measurements were run in triplicate for each biological sample, and data were normalized to total protein content, which was determined using the BCA Protein Assay Kit (Thermo Fisher Scientific, Inc., Waltham, USA).

Western blotting

Protein extraction and quantification were performed using RIPA buffer (Beyotime Biotechnology, P0013B) supplemented with protease inhibitor cocktail (Sigma-Aldrich, P8340). A total of 20 μg protein *per* sample was denatured by heating at 95°C for 5 min in Laemmli sample buffer (Bio-Rad, 1610747) containing 5% β-mercaptoethanol (Sigma-Aldrich, M6250). Proteins were separated using 10% SDS-polyacrylamide gel electrophoresis (PAGE) and transferred onto PVDF membranes (Millipore, IPVH00010) *via* electroblotting (Bio-Rad Trans-Blot Turbo system). Membranes were blocked with 5% bovine serum albumin (BSA, Sigma-Aldrich, A2153) in Tris-buffered saline containing 0.1% Tween-20 (TBST) for 1 hour at room temperature to prevent non-specific binding. Primary antibody incubation was performed overnight at 4°C with gentle agitation using the following antibodies: anti-LDHA (Cell Signaling Technology, #3582, 1:1000), anti-HK2 (Abcam, ab209847, 1:1000), anti-E2F3 (Abcam, ab50917, 1:1000), and anti-GAPDH (Abcam, ab8245, 1:5000). After washing with TBST, membranes were incubated with horseradish peroxidase (HRP)-conjugated secondary antibodies (anti-rabbit IgG, Cell Signaling Technology, #7074, 1:5000; anti-mouse IgG, Cell Signaling Technology, #7076, 1:5000) for 1 hour at room temperature. Protein signals were detected using enhanced chemiluminescence (ECL) substrate (Thermo Fisher Scientific, 32106) and visualized using a chemiluminescence imaging system (Bio-Rad ChemiDoc XRS+).

Dual-luciferase reporter assay

HEC1A and HEC1B cells were seeded in 24-well plates at a density of 5×10^4 cells *per* well and cultured for 24 hours prior to transfection. Cells were co-transfected with 50 nM of either miR-497-5p mimics (Ribobio, Guangzhou, China) or negative control (miR-NC, Ribobio) along with 500 ng of psiCHECK-2 plasmid (Promega, C8021) containing either wild-type SOX9-AS1 (WT) or mutated SOX9-AS1 (MUT) construct to assess the interaction between SOX9-AS1 and miR-497-5p. Similarly, to evaluate the interaction of E2F3 mRNA and miR-497-5p, cells were co-transfected with the same miRNA mimics or control, along with psiCHECK-2 plasmid containing either wild-type E2F3 (WT) or mutated E2F3 (MUT) sequences. Transfections were performed using Lipofectamine 3000 (Thermo Fisher Scientific, L3000015) according to the manufacturer's instructions. After 48 hours of incubation at 37°C in a 5% CO_2 atmosphere, Firefly and Renilla luciferase activities were measured using the Dual-Luciferase Reporter Assay System (Promega, E1910), and luminescence was quantified using a GloMax 20/20 luminometer (Promega). All measurements were run in triplicate for each biological sample. The relative luciferase activity was calculated as the ratio of Renilla to Firefly luciferase.

RNA-pull down assay

HEC1A and HEC1B cells (1×10^7 cells *per* assay) were harvested and lysed in 1 ml of RIP lysis buffer (20 mM Tris-HCl pH 7.5, 150 mM NaCl, 1 mM EDTA, 0.5% NP-40, 5% glycerol, supplemented with RNase inhibitor (Thermo Fisher Scientific, EO0381) and protease inhibitor cocktail (Sigma-Aldrich, P8340). Cell lysates were incubated with 50 nM of either biotin-conjugated miR-497-5p probe (Genscript, custom synthesis) or a biotin-conjugated negative control probe for 4 hours at 4°C with gentle rotation. Subsequently, 50 μl of streptavidin-coated magnetic beads (Thermo Fisher Scientific, 88816) were added to each sample and incubated for an additional 2 hours at 4°C. The bead-RNA complexes

were washed five times with RIP wash buffer (50 mM Tris-HCl pH 7.5, 300 mM NaCl, 1 mM MgCl2, 0.1% NP-40). Precipitated RNAs were isolated using 1 ml TRIzol reagent (Life Technologies, 15596026) according to the manufacturer's protocol and analyzed by RT-qPCR.

Statistics

Statistical analyses were performed using IBM SPSS Statistics version 22.0 (IBM Corp., Armonk, NY, USA). Continuous variables were compared between two groups using two-tailed unpaired Student's *t*-tests. For comparisons among multiple groups, one-way ANOVA followed by Tukey's *post-hoc* test was employed. Patient overall survival was evaluated using the Kaplan-Meier method, and differences between survival curves were assessed with the log-rank test. Results are presented as mean ± standard deviation (SD) of three independent experiments. A p-value < 0.05 was considered statistically significant for all analyses.

Results

SOX9-AS1 is a potential carcinogenetic factor in EC patients with prognostic value

To investigate the relationship between SOX9-AS1 expression levels and clinical features in EC patients, we analyzed the SOX9-AS1 expression profile in primary uterine corpus endometrial carcinoma (UCEC) patients from the TCGA database. Our analysis revealed that SOX9-AS1 expression levels in primary UCEC tissues (n = 551) were significantly higher than those of normal tissues (n = 35) (Fig. 1A; p < 0.01). Furthermore, we evaluated the prognostic value of SOX9-AS1 expression levels in UCEC patients using the Kaplan-Meier method. After dividing UCEC patients into high expression and low/medium expression groups based on the median SOX9-AS1 expression, we found that UCEC patients with high SOX9-AS1 expression levels showed significantly decreased survival probability compared to those with low/medium SOX9-AS1 expression levels (Fig. 1B). This finding indicates the clinical significance of SOX9-AS1 expression in EC patients. Moreover, the upregulation of SOX9-AS1 was validated in EC cell lines by RT-qPCR, which demonstrated significantly higher levels of SOX9-AS1 expressions in different EC cell lines (HEC1A, HEC1B, Ishikawa, RL95-2, and KLE) compared to human normal endometrial fibroblast cells (HESCs) (Fig. 1C).

SOX9-AS1 knockdown inhibits proliferation, mobility and glycolysis of EC cells

To explore the function of SOX9-AS1 in regulating the aggressiveness of EC cells, we performed knockdown experiments in HEC1A and HEC1B cells which showed the highest SOX9-AS1 expression levels. We used four different shRNAs specifically targeting SOX9-AS1 (sh-SOX9-AS1 #1, sh-SOX9-AS1 #2, sh-SOX9-AS1 #3, or sh-SOX9-AS1 #4) and validated the knockdown efficiency using qRT-PCR assay. The sh-SOX9-AS1 #1 showed the strongest knockdown efficacy, with relative SOX9-AS1 expression levels reduced to about 25% compared to the negative control (sh-NC) (Fig. 2A). Consequently, sh-SOX9-AS1 #1 was selected as the standard sh-SOX9-AS1 for subsequent experiments.

The effect of SOX9-AS1 knockdown on the proliferation of EC cells was assessed using CCK-8 assay and EdU incor-

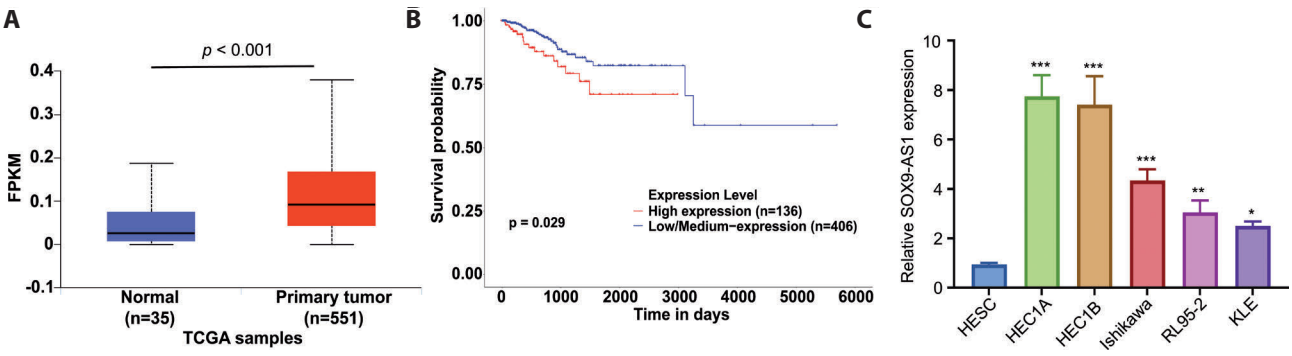

Figure 1. SOX9-AS1 is upregulated in EC tissues and cells, correlating with poor overall survival in EC patients. **A.** SOX9-AS1 expression in EC tissues (n = 551) *versus* normal tissues (n = 35) based on TCGA database. FPKM, Fragments Per Kilobase of exon *per* Million mapped reads (a method used to normalize gene expression data obtained from RNA sequencing). **B.** Kaplan-Meier curve of overall survival in uterine corpus endometrial carcinoma (UCEC) patients with high (n = 136) or low/medium (n = 406) SOX9-AS1 expression. **C.** SOX9-AS1 expression in EC cell lines (HEC1A, HEC1B, Ishikawa, RL95-2, and KLE) *versus* human normal endometrial fibroblast cells (HESCs) determined by qRT-PCR. GAPDH served as internal reference. * p < 0.05, ** p < 0.01, and *** p < 0.001.

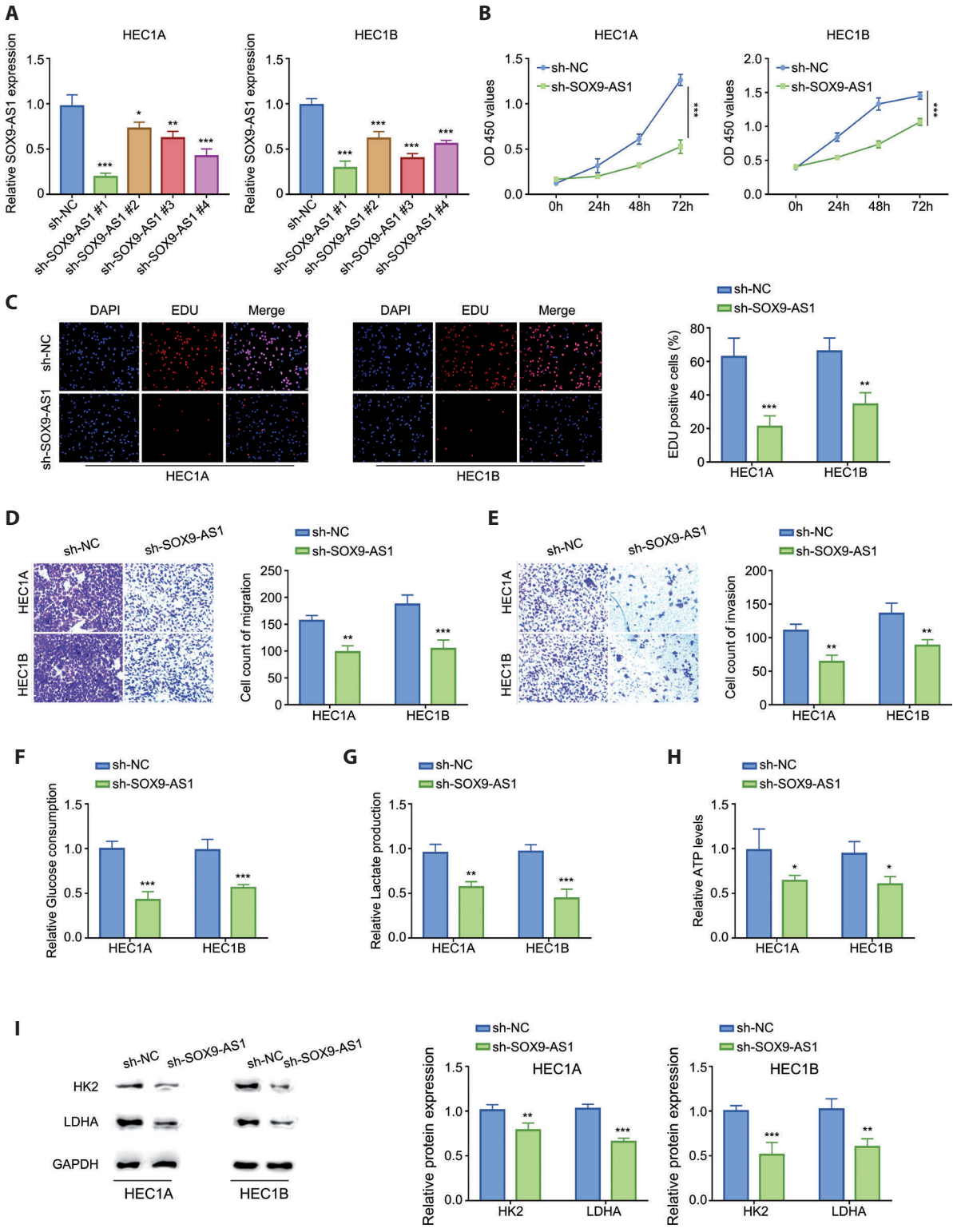

Figure 2. SOX9-AS1 knockdown inhibits proliferation, migration, invasion, and glycolysis of EC cells. **A.** qRT-PCR confirmation of SOX9-AS1 knockdown in HEC1A and HEC1B cells using four shRNAs. HEC1A and HEC1B cells were introduced with control sh-RNA or sh-SOX9-AS1 #1. **B.** Cell proliferation assessed by CCK-8 assay. **C.** Cell proliferation evaluated by Edu incorporation assay. **D.** Cell migration measured by wound healing assay. **E.** Cell invasion assessed by Transwell assay. Glycolysis-related measurements: glucose uptake (**F**), lactate production (**G**), and ATP production (**H**). **I.** Protein levels of key glycolytic enzymes (HK2, and LDHA) assessed by Western blot. * $p < 0.05$, ** $p < 0.01$, and *** $p < 0.001$.

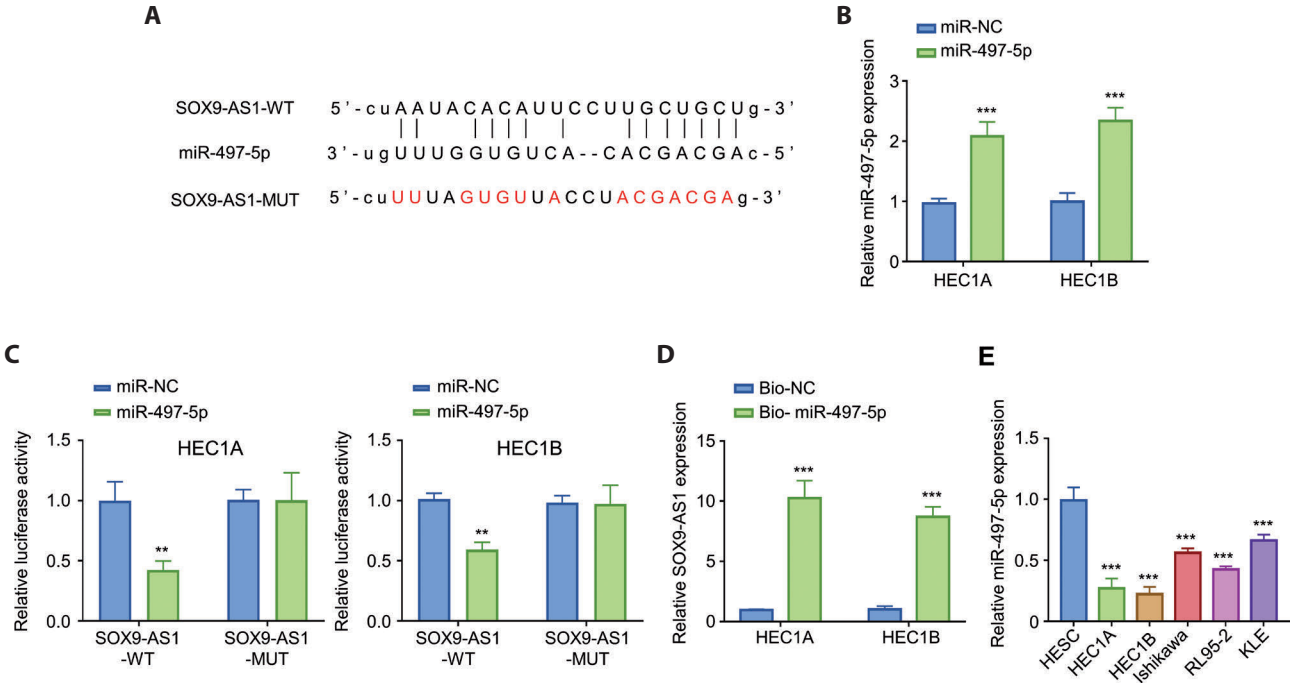

Figure 3. SOX9-AS1 acts as a sponge for miR-497-5p. **A.** Predicted miR-497-5p binding sites on SOX9-AS1 using starBase database. **B.** miR-497-5p expression in HEC1A and HEC1B cells after transfection with miR-497-5p mimics, measured by qRT-PCR. **C.** Dual-luciferase reporter assay using wild-type and mutant SOX9-AS1 constructs. **D.** RNA pull-down assay confirming SOX9-AS1-miR-497-5p interaction. **E.** miR-497-5p expression in EC cell lines *versus* HESCs, determined by qRT-PCR. ** $p < 0.01$, and *** $p < 0.001$.

poration assay in HEC1A and HEC1B cells with SOX9-AS1 shRNA expression. The results demonstrated that knockdown of SOX9-AS1 significantly inhibited proliferation in both HEC1A and HEC1B cells compared to the negative control cells (Fig. 2B,C). Additionally, we investigated the impacts of SOX9-AS1 knockdown on the migratory and invasive capabilities of HEC1A and HEC1B cells. SOX9-AS1 knockdown significantly reduced cell migration (Fig. 2D) and invasion (Fig. 2E). To further elucidate the effect of SOX9-AS1 silencing on cell metabolism, we analyzed glucose consumption, lactate production, and ATP levels influenced upon SOX9-AS1 silencing. We found that SOX9-AS1 knockdown significantly decreased glucose consumption (Fig. 2F), lactate production (Fig. 2G), and ATP levels (Fig. 2H). Meanwhile, the protein expression levels of HK2 and LDHA (two key enzymes involved in glycolysis) were significantly reduced by SOX9-AS1 knockdown (Fig. 2I). Collectively, these findings suggest that SOX9-AS1 plays a critical role in regulating the malignancy of EC cells and maintaining glycolysis.

SOX9-AS1 serves as a sponge of miR-497-5p in EC cells

To investigate the mechanism of SOX9-AS1, specifically to determine whether it could act as a sponge for miRNAs, we performed bioinformatics prediction using starBase online tool (http://starbase.sysu.edu.cn). Our analysis identified miR-497-5p as a potential target of SOX9-AS1 (Fig. 3A). To validate their interaction, we applied miR-497-5p mimics to over-express miR-497-5p in HEC1A and HEC1B cells (Fig. 3B). Subsequently, we conducted dual-luciferase reporter and RNA pull-down assays to verify the interaction between SOX9-AS1 and miR-497-5p. Our findings revealed that co-transfection of the miR-497-5p mimics resulted in a marked reduction in the luciferase activity of the wild-type SOX9-AS1 reporter, an effect that was nullified when the predicted binding sites between SOX9-AS1 and miR-497-5p were mutated (Fig. 3C). Biotin-conjugated miR-497-5p probe (Bio-miR-497-5p) was also found to precipitate a greater amount of SOX9-AS1 compared to the negative control probe (Bio-NC) in both HEC1A and HEC1B cell lines (Fig. 3D), indicating their physical interaction. Interestingly, miR-497-5p expression was significantly lower in EC cell lines (HEC1A, HEC1B, Ishikawa, RL95-2, and KLE) relative to HESCs (Fig. 3E). Therefore, these data suggest that SOX9-AS1 may act as a molecular sponge to suppress miR-497-5p activity.

SOX9-AS1 promotes proliferation, migration, invasion and glycolysis in EC cells by targeting miR-497-5p

To investigate whether SOX9-AS1 promotes the malignant phenotype of EC cells through the sponging of miR-497-5p,

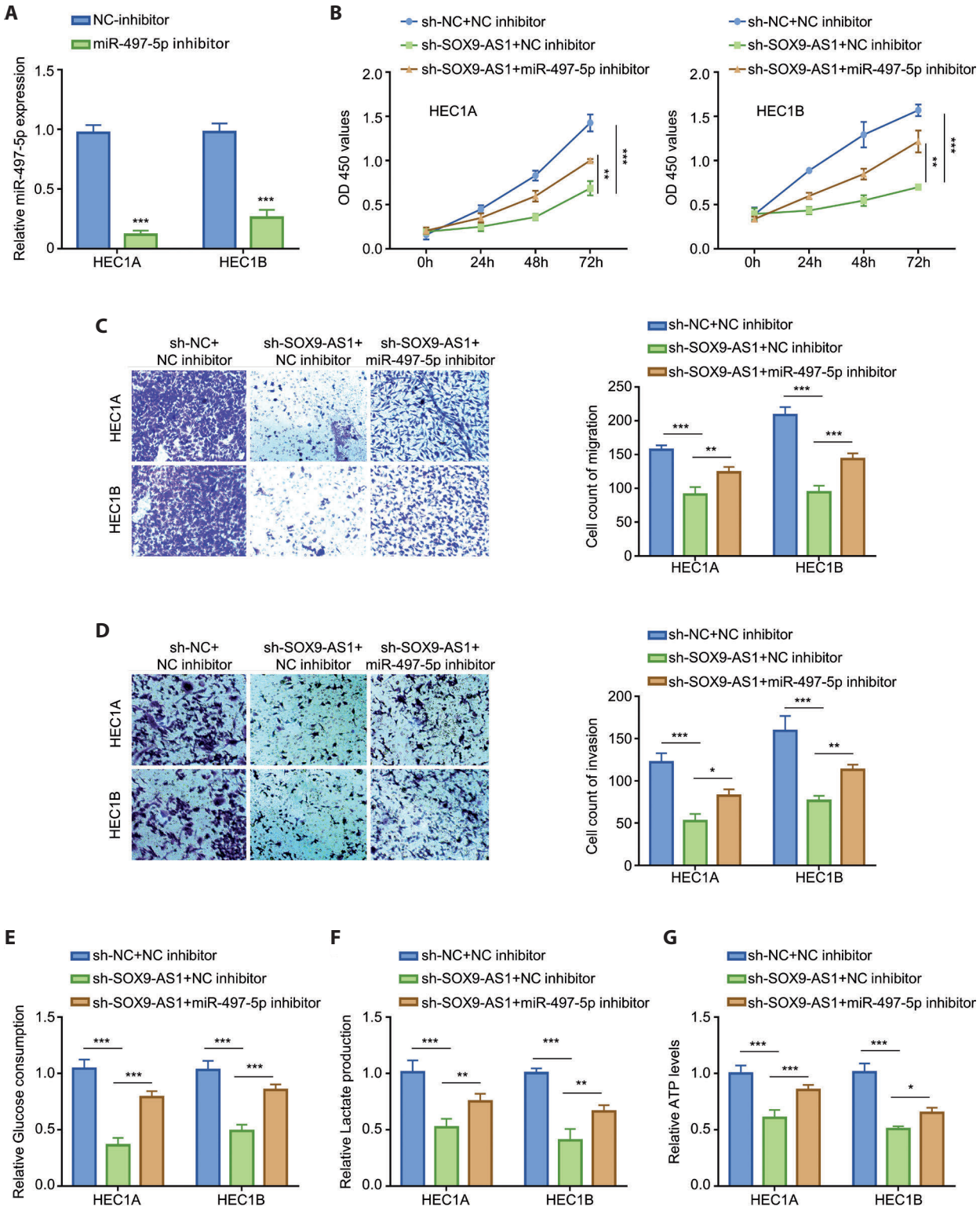

Figure 4. SOX9-AS1 promotes EC cell proliferation, migration, invasion, and glycolysis by targeting miR-497-5p. **A.** Efficiency of miR-497-5p inhibitor in HEC1A and HEC1B cells, assessed by qRT-PCR. **B.** Cell proliferation measured by CCK-8 assay. **C.** Cell migration evaluated by wound healing assay. **D.** Cell invasion assessed by Transwell assay. Glycolysis levels measured by: glucose uptake (**E**), lactate production (**F**) and ATP production (**G**) in HEC1A and HEC1B cells after SOX9-AS1 knockdown with or without miR-497-5p inhibition (sh-NC+NC inhibitor, sh-SOX9-AS1+NC inhibitor, sh-SOX9-AS1+miR-497-5p inhibitor). * $p < 0.05$, ** $p < 0.01$, and *** $p < 0.001$.

rescue experiments were conducted by applying synthetic miR-497-5p inhibitor together with knockdown of SOX9-AS1 (experimental grouping: sh-NC combined with NC inhibitor, sh-SOX9-AS1 along with NC inhibitor, and sh-SOX9-AS1 together with miR-497-5p inhibitor). Following the successful suppression of miR-497-5p levels by miR-497-5p inhibitor in HEC1A and HEC1B cells (Fig. 4A), cell proliferation, migration, invasion, and glycolysis level were evaluated. SOX9-AS1-knockdown (sh-SOX9-AS1+NC inhibitor) suppressed cell proliferation (Fig. 4B), migration (Fig. 4C), and invasion (Fig. 4D), which was concomitant with reductions in glucose consumption (Fig. 4E), lactate production (Fig. 4F) and the cellular ATP levels (Fig. 4G). Simultaneous inhibition of miR-497-5p by co-transfecting miR-497-5p inhibitor (sh-SOX9-AS1+miR-497-5p inhibitor) partially reversed all these changes induced by SOX9-AS1-knockdown (Fig. 4B–G). These results suggest that the role of SOX9-AS1 in regulating aggressiveness of EC cells is mediated at least partially through targeting miR-497-5p.

SOX9-AS1 acts as a competitive endogenous RNA (ceRNA) of miR-497-5p to increase E2F3 expression in EC cells

To delve deeper into the ceRNA network involving SOX9-AS1, a bioinformatics analysis was conducted to predict the downstream mRNA targets of miR-497-5p utilizing the starbase tool (http://starbase.sysu.edu.cn). This analysis showed that miR-497-5p harbors complementary sequences with the 3'untranslated region (UTR) E2F3 mRNA (Fig. 5A). Following this, a Dual-Luciferase reporter assay was conducted to verify the specific interaction between miR-497-5p and the E2F3-3'UTR. The wild-type E2F3-3'UTR (E2F3-WT) reporter demonstrated over a 50% reduction in reporter activity after miR-497-5p overexpression, whereas the mutated E2F3-3'UTR (E2F3-MUT) reporter did not exhibit significant inhibition (Fig. 5B). Furthermore, we assessed the expression levels of E2F3 in EC cells with elevated miR-497-5p levels. The results indicated that the overexpression of miR-497-5p

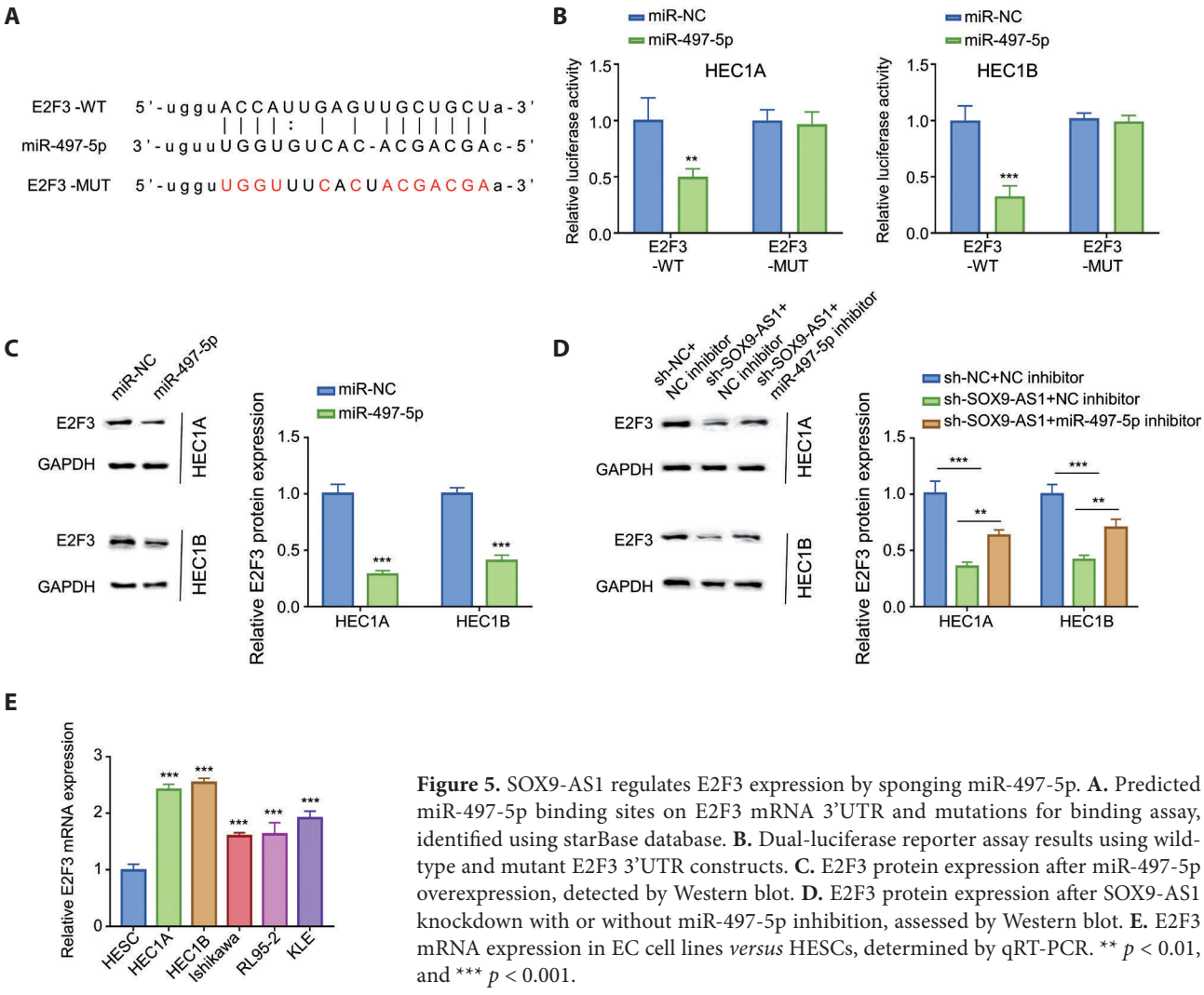

Figure 5. SOX9-AS1 regulates E2F3 expression by sponging miR-497-5p. **A.** Predicted miR-497-5p binding sites on E2F3 mRNA 3'UTR and mutations for binding assay, identified using starBase database. **B.** Dual-luciferase reporter assay results using wild-type and mutant E2F3 3'UTR constructs. **C.** E2F3 protein expression after miR-497-5p overexpression, detected by Western blot. **D.** E2F3 protein expression after SOX9-AS1 knockdown with or without miR-497-5p inhibition, assessed by Western blot. **E.** E2F3 mRNA expression in EC cell lines *versus* HESCs, determined by qRT-PCR. ** $p < 0.01$, and *** $p < 0.001$.

significantly decreased E2F3 expression in both HEC1A and HEC1B cell lines (Fig. 5C). Further analyses demonstrated that the knockdown of SOX9-AS1 (sh-SOX9-AS1 along with the NC inhibitor) led to a reduction in E2F3 levels in HEC1A and HEC1B cells. This reduction was partially counteracted by inhibiting miR-497-5p through co-transfection with a miR-

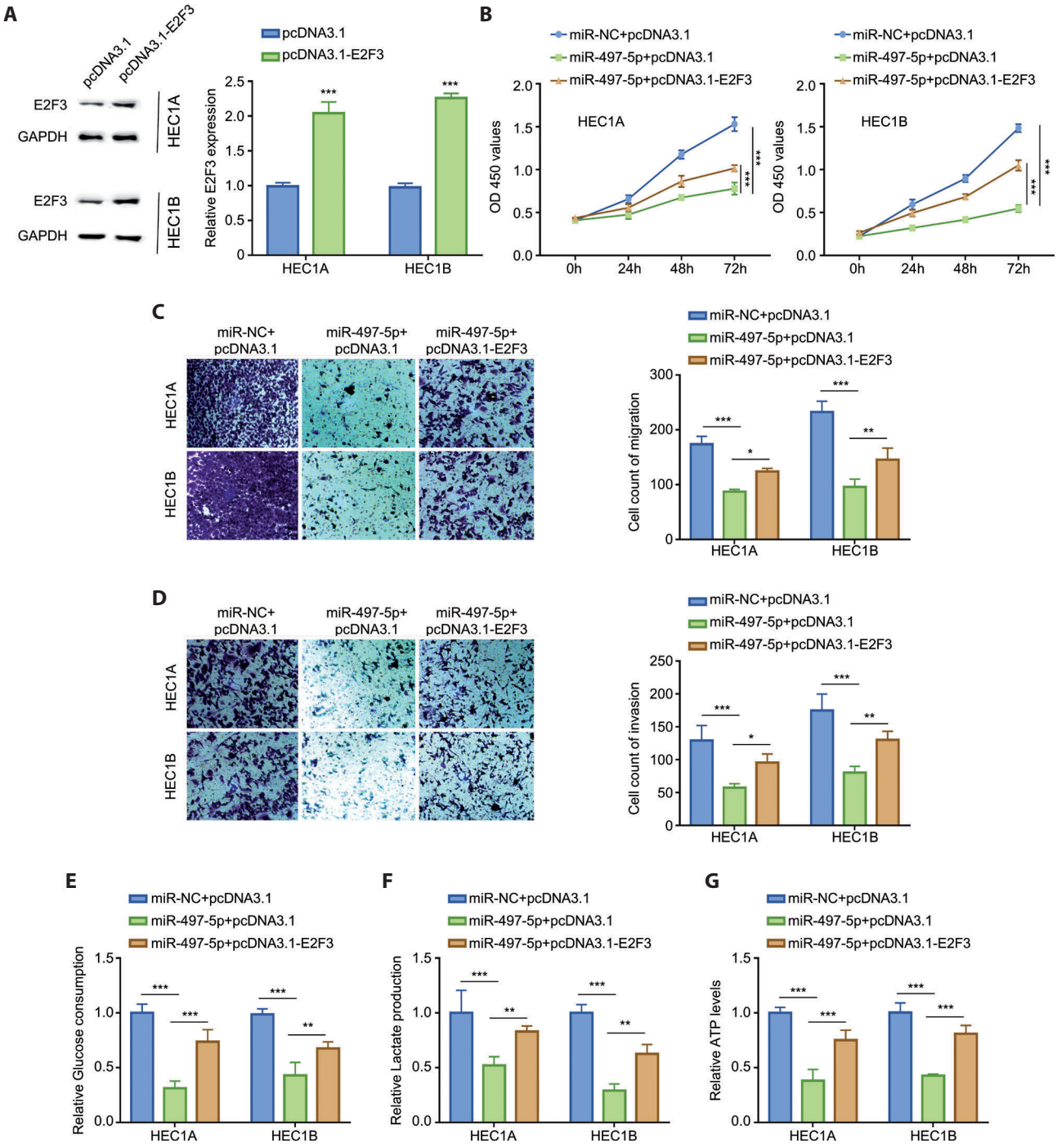

Figure 6. miR-497-5p inhibits EC cell proliferation, migration, invasion, and glycolysis by targeting E2F3. **A.** E2F3 overexpression efficiency in HEC1A and HEC1B cells, confirmed by Western blot. **B.** Cell proliferation assessed by CCK-8 assay. **C.** Cell migration evaluated by wound healing assay. **D.** Cell invasion measured by Transwell assay. Glycolysis levels measured by: glucose uptake (**E**), lactate production (**F**) and ATP production (**G**) after miR-497-5p overexpression with or without E2F3-overexpression in HEC1A and HEC1B cells (miR-NC+pcDNA3.1, miR-497-5p+pcDNA3.1, miR-497-5p+pcDNA3.1-E2F3). * $p < 0.05$, ** $p < 0.01$, and *** $p < 0.001$.

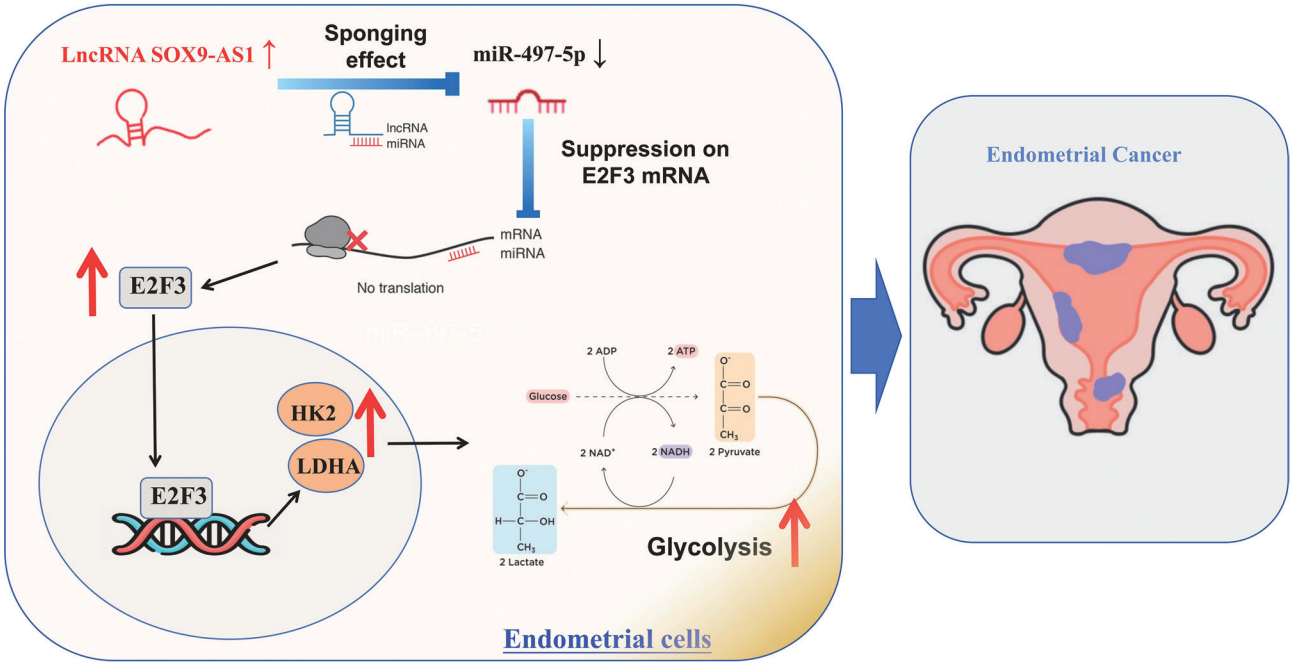

Figure 7. A schematic drawing of the current study.

497-5p inhibitor (sh-SOX9-AS1 combined with the miR-497-5p inhibitor) (Fig. 5D). Furthermore, a significant increase in E2F3 expression was observed in EC cell lines (HEC1A, HEC1B, Ishikawa, RL95-2, and KLE) when compared to HESCs (Fig. 5E).

Moreover, rescue experiments were carried out by miR-497-5p mimic transfection, with and without concurrent overexpression of E2F3 (miR-NC+pcDNA3.1, miR-497-5p+pcDNA3.1, miR-497-5p+pcDNA3.1-E2F3). E2F3 overexpression in HEC1A and HEC1B cells was successfully achieved via the transfection of pcDNA3.1-E2F3 expression vector (Fig. 6A). We found that overexpression of miR-497-5p (miR-497-5p+pcDNA3.1) led to reductions in cell proliferation (Fig. 6B), migration (Fig. 6C), and invasion (Fig. 6D), as well as the suppression in glucose consumption (Fig. 6E), lactate production (Fig. 6F), and ATP levels (Fig. 6G). Simultaneous E2F3 overexpression in these cells (miR-497-5p+pcDNA3.1-E2F3) partially reversed the alterations induced by miR-497-5p overexpression (Fig. 6B–G). Together, our findings indicate that SOX9-AS1 acts as a ceRNA of miR-497-5p to increase E2F3 expression in EC cells.

Discussion

EC represents a prevalent form of gynecological cancer, with a notable rise in both incidence and mortality rates (Gupta 2017; Bray et al. 2018). LncRNAs have demonstrated significant involvement in various processes of cancer initiation and advancement, including EC (Wang et al. 2021; Zhang et al. 2022). The lncRNA known as SOX9-AS1 has been found to be upregulated across multiple cancer types, where it facilitates cell proliferation and invasion (Sun et al. 2020; Zhou et al. 2020; Wu et al. 2022; Huang et al. 2023). Moreover, discovering and characterizing lncRNAs that contribute to the progression of EC could enhance our comprehension of the disease's biological mechanisms and aid in the formulation of innovative diagnostic and treatment strategies. Nonetheless, the specific functions and molecular pathways associated with SOX9-AS1 in EC are still not well elucidated. In the present study, we carried out a thorough investigation to explore the function and molecular mechanisms of SOX9-AS1 in the progression of EC, a prevalent gynecological malignancy and a significant global health issue with largely unclear molecular pathogenesis (Gupta 2017; Bray et al. 2018).

Initially, we examined the expression pattern and functional engagement of SOX9-AS1 in EC. We reported SOX9-AS1 as a significant factor involved in the progression of EC, since SOX9-AS1 exhibited elevated expression levels in both EC tissues and cell lines, and SOX9-AS1 knockdown suppressed proliferation, migration, invasion, and glycolysis in EC cells. Importantly, high expression of SOX9-AS1 was notably linked to unfavorable outcomes in patients diagnosed with EC. This finding indicates the clinical significance of SOX9-AS1 expression in the prognosis in EC patients. Our findings align with and extend previous studies on SOX9-AS1's oncogenic roles. In triple-negative

breast cancer, SOX9-AS1 was shown to drive lipid metabolic reprogramming alongside promoting cell migration and invasion (Cisneros-Villanueva et al. 2024), suggesting its diverse regulatory roles in cancer metabolism. Similar to our results, SOX9-AS1 demonstrates oncogenic properties in hepatocellular carcinoma through a positive feedback loop mechanism (Zhang et al. 2019). These studies collectively support SOX9-AS1's role as an oncogenic lncRNA across different cancer types, particularly in regulating cancer cell metabolism and progression.

Our findings highlight the significant role of SOX9-AS1/miR-497-5p axis in the progression of EC. SOX9-AS1 was found to be upregulated in EC tissues and cell lines, while miR-497-5p showed downregulation. SOX9-AS1 was found to functionally and physically interact with miR-497-5p. The sponging effect of SOX9-AS1 suppressed the tumor suppressor activity of miR-497-5p in EC. These results indicate that SOX9-AS1 and miR-497-5p play opposing roles in EC development, with SOX9-AS1 promoting tumor progression and miR-497-5p showing suppressive effect. The tumor-suppressive role of miR-497-5p observed in our study is consistent with previous findings across multiple cancer types. miR-497-5p has been shown to inhibit tumor growth and invasion by targeting SRY-box transcription factor 5 (SOX5) in non-small-cell lung cancer (Li et al. 2019), suppress osteosarcoma growth by targeting ADP-ribosylation factor-like protein 2 (ARL2) (Sun et al. 2017), and regulate fibroblast growth factor 2 (FGF2) to inhibit NSCLC proliferation and invasion (Huang et al. 2019). Similarly, studies have demonstrated miR-497-5p's inhibitory effects on cell proliferation and invasion in angiosarcoma through calcium-activated potassium channel 3.1 (KCa3.1) targeting (Chen et al. 2016) and in gastric cancer *via* pyruvate dehydrogenase kinase 3 (PDK3) regulation (Feng et al. 2019). Our results reveal that SOX9-AS1 functionally sponges miR-497-5p, thereby suppressing its tumor-suppressive activity in EC. The functional interplay between these molecules presents potential therapeutic targets for EC treatment.

Further investigation into the molecular mechanisms revealed a complex interplay between SOX9-AS1, miR-497-5p, and E2F3 in EC. The study demonstrated E2F3 as a target of miR-497-5p. This sponging effect of SOX9-AS1 on miR-497-5p leads to an increase in E2F3 expression. E2F3, known for its oncogenic properties, was shown to promote the malignant phenotype of EC cells. This SOX9-AS1/miR-497-5p/E2F3 axis represents a novel regulatory mechanism in EC progression, where SOX9-AS1 indirectly upregulates E2F3 by sequestering miR-497-5p. E2F3 amplification and overexpression have been well-documented in various cancers, including bladder cancer where it associates with invasive tumor growth and rapid proliferation (Feber et al. 2004; Oeggerli et al. 2004). High E2F3 expression has been identified as an independent predictor of poor clinical outcome in prostate cancer (Foster et al. 2004) and serves as a negative prognostic marker in neuroblastoma (Parodi et al. 2020; Ognibene et al. 2022) The oncogenic role of E2F3 is further supported by its function in modulating cellular proliferation in bladder and prostate cancer cells (Olsson et al. 2007). Notably, E2F3 has been implicated in metabolic regulation, including its role in the CDK4-E2F3 pathway affecting metabolism (Bahn et al. 2023) and its involvement in promoting glycolysis in non-small cell lung cancer (Yan et al. 2022). These findings collectively establish E2F3 as a crucial oncogenic driver that promotes tumor progression across multiple cancer types.

While our study provides valuable insights into the SOX9-AS1/miR-497-5p/E2F3 axis in EC, several limitations should be acknowledged. The primary focus on *in vitro* experiments, while informative, may not fully reflect the complex tumor microenvironment present *in vivo*. Further *in vivo* studies and clinical investigations are necessary to validate these findings and establish their relevance in larger cohorts of EC patients. The relationship between SOX9-AS1 expression and therapeutic response remains to be explored, including its potential role as a predictive biomarker for specific treatments, its impact on chemotherapy sensitivity, and its utility in treatment stratification. Additionally, while we demonstrated this regulatory axis in EC, future studies should investigate whether this mechanism can be generalized to other cancer types, which would require comprehensive molecular and functional validation in different cancer contexts. The therapeutic potential of targeting SOX9-AS1 requires extensive preclinical and clinical testing to assess efficacy and safety. Future research should also consider a more comprehensive approach to elucidate other key players and regulatory pathways in EC progression, as well as explore the broader metabolic consequences of SOX9-AS1 upregulation.

In conclusion, our study provides important insights into the molecular mechanisms of EC development, revealing a novel regulatory axis involving SOX9-AS1, miR-497-5p, and E2F3 (Fig. 7). These findings suggest that targeting this axis, particularly SOX9-AS1, may offer promising therapeutic strategies for EC intervention. Future *in vivo* studies and clinical investigations are necessary to validate these findings and explore their potential as therapeutic targets.

Data and material availability. Data used or analyzed in this work can be obtained from corresponding author upon request.

Conflict of interest. The authors claim no competing interests.

Authors' contributions. BJ Zeng, LM Lai, JJ Lin and MY Li contributed to literature review, study design, manuscript writing and critical revision, and preparation of Figures 1–3. XL Ren and YL Cheng was in charge of data extraction, analysis and interpretation, and preparation of Figures 4–6. All authors read and agreed to this eventual version for publication.

References

Bahn YJ, Yadav H, Piaggi P, Abel BS, Gavrilova O, Springer DA, Papazoglou I, Zerfas PM, Skarulis MC, McPherron AC, Rane SG (2023): CDK4-E2F3 signals enhance oxidative skeletal muscle fiber numbers and function to affect myogenesis and metabolism. J. Clin. Invest. **133,** e162479 https://doi.org/10.1172/JCI162479

Barba I, Carrillo-Bosch L, Seoane J (2024): Targeting the Warburg effect in cancer: Where do we stand? Int. J. Mol. Sci. **25,** 3142 https://doi.org/10.3390/ijms25063142

Bray F, Ferlay J, Soerjomataram I, Siegel RL, Torre LA, Jemal A (2018): Global cancer statistics 2018: GLOBOCAN estimates of incidence and mortality worldwide for 36 cancers in 185 countries. CA Cancer J. Clin. **68,** 394-424 https://doi.org/10.3322/caac.21492

Cao X, Ma Q, Wang B, Qian Q, Xi Y (2022): Circ-E2F3 promotes cervical cancer progression by inhibiting microRNA-296-5p and increasing STAT3 nuclear translocation. Ann. N.Y. Acad. Sci. **1507,** 84-98 https://doi.org/10.1111/nyas.14653

Chen Y, Kuang D, Zhao X, Chen D, Wang X, Yang Q, Wan J, Zhu Y, Wang Y, Zhang S, et al. (2016): miR-497-5p inhibits cell proliferation and invasion by targeting KCa3.1 in angiosarcoma. Oncotarget **7,** 58148-58161 https://doi.org/10.18632/oncotarget.11252

Cisneros-Villanueva M, Fonseca-Montaño MA, Ríos-Romero M, López-Camarillo C, Jiménez-Morales S, Langley E, Rosette-Rueda AS, Cedro-Tanda A, Hernández-Sotelo D, Hidalgo-Miranda A (2024): LncRNA SOX9-AS1 triggers a transcriptional program involved in lipid metabolic reprogramming, cell migration and invasion in triple-negative breast cancer. Sci. Rep. **14,** 1483 https://doi.org/10.1038/s41598-024-51947-2

Crosbie EJ, Kitson SJ, McAlpine JN, Mukhopadhyay A, Powell ME, Singh N (2022): Endometrial cancer. Lancet **399,** 1412-1428 https://doi.org/10.1016/S0140-6736(22)00323-3

Feber A, Clark J, Goodwin G, Dodson AR, Smith PH, Fletcher A, Edwards S, Flohr P, Falconer A, Roe T (2004): Amplification and overexpression of E2F3 in human bladder cancer. Oncogene **23,** 1627-1630 https://doi.org/10.1038/sj.onc.1207274

Feng L, Cheng K, Zang R, Wang Q, Wang J (2004): miR-497-5p inhibits gastric cancer cell proliferation and growth through targeting PDK3. Biosci. Rep. **39,** BSR20190654 https://doi.org/10.1042/BSR20190654

Foster CS, Falconer A, Dodson AR, Norman AR, Dennis N, Fletcher A, Southgate C, Dowe A, Dearnaley D, Jhavar S, et al. (2004): Transcription factor E2F3 overexpressed in prostate cancer independently predicts clinical outcome. Oncogene **23,** 5871-5879 https://doi.org/10.1038/sj.onc.1207800

Ganapathy-Kanniappan S, Geschwind JF (2013): Tumor glycolysis as a target for cancer therapy: progress and prospects. Mol. Cancer **12,** 152 https://doi.org/10.1186/1476-4598-12-152

Gonzalez-Bosquet J, Gabrilovich S, McDonald ME, Smith BJ, Leslie KK, Bender DD, Goodheart MJ, Devor E (2022): Integration of genomic and clinical retrospective data to predict endometrioid endometrial cancer recurrence. Int. J. Mol. Sci. **23,** 16014 https://doi.org/10.3390/ijms232416014

Gupta D (2017): Clinical behavior and treatment of endometrial cancer. Adv. Exp. Med. Biol. **943,** 47-74 https://doi.org/10.1007/978-3-319-43139-0_2

He D, Chen M, Chang L, Gu J, Liu F, Gao X, Ruan Y (2022): De novo pyrimidine synthesis fuels glycolysis and confers chemoresistance in gastric cancer. Cancer Lett. **549,** 215837 https://doi.org/10.1016/j.canlet.2022.215837

Huang H, Yan J, Lan X, Guo Y, Sun M, Zhao Y, Zhang F, Sun J, Lu S (2023): LncRNA WDR11-AS1 promotes extracellular matrix synthesis in osteoarthritis by directly interacting with RNA-binding protein PABPC1 to stabilize SOX9 expression. Int. J. Mol. Sci. **24,** 817 https://doi.org/10.3390/ijms24010817

Huang X, Wang L, Liu W, Li F (2019): MicroRNA-497-5p inhibits proliferation and invasion of non-small cell lung cancer by regulating FGF2. Oncol. Lett. **17,** 3425-3431 https://doi.org/10.3892/ol.2019.9954

Li G, Wang K, Wang J, Qin S, Sun X, Ren H (2019): miR-497-5p inhibits tumor cell growth and invasion by targeting SOX5 in non-small-cell lung cancer. J. Cell. Biochem. **120,** 10587-10595 https://doi.org/10.1002/jcb.28345

Lv C, Sun J, Ye Y, Lin Z, Li H, Liu Y, Mo K, Xu W, Hu W, Draz E, Wang S (2022): Long noncoding RNA EIF1AX-AS1 promotes endometrial cancer cell apoptosis by affecting EIF1AX mRNA stabilization. Cancer Sci. **113,** 1277-1291 https://doi.org/10.1111/cas.15275

Makker V, MacKay H, Ray-Coquard I, Levine DA, Westin SN, Aoki D, Oaknin A (2021): Endometrial cancer. Nat. Rev. Dis. Primers **7,** 88 https://doi.org/10.1038/s41572-021-00324-8

Nie C, Han J, Bi W, Qiu Z, Chen L, Yu J, Pang R, Liu B, Sheng R, Zhang J (2022): Circular RNA circ_0000644 promotes papillary thyroid cancer progression via sponging miR-1205 and regulating E2F3 expression. Cell Cycle **21,** 126-139 https://doi.org/10.1080/15384101.2021.2012334

Oeggerli M, Tomovska S, Schraml P, Calvano-Forte D, Schafroth S, Simon R, Gasser T, Mihatsch MJ, Sauteret G (2004): E2F3 amplification and overexpression is associated with invasive tumor growth and rapid tumor cell proliferation in urinary bladder cancer. Oncogene **23,** 5616-5623 https://doi.org/10.1038/sj.onc.1207749

Ognibene M, Cangelosi D, Sorrentino S, Zanardi S, Zara F, Pezzolo A, Parodi S (2022): E2F3 gene expression is a potential negative prognostic marker for localised and MYCN not-amplified neuroblastoma: Results of in silico analysis of 786 samples. Pediatr. Blood Cancer **69,** e29800 https://doi.org/10.1002/pbc.29800

Olsson AY, Feber A, Edwards S, Te Poele R, Giddings I, Merson S, Cooper CS (2007): Role of E2F3 expression in modulating cellular proliferation rate in human bladder and prostate cancer cells. Oncogene **26,** 1028-1037 https://doi.org/10.1038/sj.onc.1209854

Parodi S, Ognibene M, Haupt R, Pezzolo A (2020): The overexpression of E2F3 might serve as prognostic marker for

neuroblastoma patients with stage 4S disease. Diagnostics (Basel) **10,** 315
https://doi.org/10.3390/diagnostics10050315

Shan L, Lu Y, Xiang CC, Zhu X, Zuo ED, Cheng X (2022): Identification of five m6A-related lncRNA genes as prognostic markers for endometrial cancer based on TCGA database. J. Immunol. Res. **2022,** 2547029
https://doi.org/10.1155/2022/2547029

Sun T, Liu Z, Zhang R, Ma S, Lin T, Li Y, Yang S, Zhang W, Wang Y (2020): Long non-coding RNA LEF1-AS1 promotes migration, invasion and metastasis of colon cancer cells through miR-30-5p/SOX9 axis. Onco. Targets Ther. **13,** 2957-2972
https://doi.org/10.2147/OTT.S232839

Sun Z, Li A, Yu Z, Li X, Guo X, Chen R (2017): MicroRNA-497-5p suppresses tumor cell growth of osteosarcoma by targeting ADP ribosylation factor-like protein 2. Cancer Biother. Radiopharm. **32,** 371-378
https://doi.org/10.1089/cbr.2017.2268

Vander Heiden MG, Cantley LC, Thompson CB (2009): Understanding the Warburg effect: the metabolic requirements of cell proliferation. Science **324,** 1029-1033
https://doi.org/10.1126/science.1160809

Wang J, Lei C, Shi P, Teng H, Lu L, Guo H, Wang X (2021): LncRNA DCST1-AS1 promotes endometrial cancer progression by modulating the miR-665/HOXB5 and miR-873-5p/CADM1 pathways. Front. Oncol. **11,** 714652
https://doi.org/10.3389/fonc.2021.714652

Wu L, Yang J, Ke RS, Liu Y, Guo P, Feng L, Li Z (2022): Impact of lncRNA SOX9-AS1 overexpression on the prognosis and progression of intrahepatic cholangiocarcinoma. Clin. Res. Hepatol. Gastroenterol. **46,** 101999
https://doi.org/10.1016/j.clinre.2022.101999

Wu XP, Xu ZQ, Xie WM, Lai YL, He K, Jiang Y, Xu ZC, Lin YN, Xie YF (2022): Long non-coding RNA GAS6-AS1 enhances breast cancer cell aggressiveness by functioning as a competing endogenous RNA of microRNA-215-5p to enhance SOX9 expression. Exp. Ther. Med. **23,** 109
https://doi.org/10.3892/etm.2021.11032

Yan X, Wang T, Wang J (2022): Circ_0016760 acts as a sponge of microRNA-4295 to enhance E2F transcription factor 3 expression and facilitates cell proliferation and glycolysis in non-small cell lung cancer. Cancer Biother. Radiopharm. **37,** 147-158
https://doi.org/10.1089/cbr.2020.3621

Zhang HQ, Li T, Li C, Hu HT, Zhu SM, Lu JQ, Chen XJ, Huang HF, Wu YT (2022): LncRNA THOR promotes endometrial cancer progression through the AKT and ERK signaling pathways. Med. Oncol. **39,** 207
https://doi.org/10.1007/s12032-022-01802-z

Zhang W, Wu Y, Hou B, Wang Y, Deng D, Fu Z, Xu Z (2019): A SOX9-AS1/miR-5590-3p/SOX9 positive feedback loop drives tumor growth and metastasis in hepatocellular carcinoma through the Wnt/β-catenin pathway. Mol. Oncol. **13,** 2194-2210
https://doi.org/10.1002/1878-0261.12560

Zhao W, Zhu X, Jin Q, Lin B, Ji R (2022): The lncRNA NEAT1/miRNA-766-5p/E2F3 regulatory axis promotes prostate cancer progression. J. Oncol. **2022,** 1866972
https://doi.org/10.1155/2022/1866972

Zhou T, Wu L, Ma N, Tang F, Yu Z, Jiang Z, Li Y, Zong Z, Hu K (2020): SOX9-activated FARSA-AS1 predetermines cell growth, stemness, and metastasis in colorectal cancer through upregulating FARSA and SOX9. Cell Death Dis. **11,** 1071
https://doi.org/10.1038/s41419-020-03273-4

Received: June 5, 2024
Final version accepted: April 2, 2025